JOURNAL OF MATERIALS SCIENCE 30 (1995) 465–472

Thermal cycling of iridium coatings on isotropic graphite

K. MUMTAZ, J. ECHIGOYA, H. ENOKI, T. HIRAI*, Y. SHINDO
*Department of Materials Processing, Faculty of Engineering, and *Institute for Materials Research, Tohoku University, Sendai-980, Japan*

The surface morphology observed on the iridium-coated isotropic graphite substrate varied widely between 300 and up to 2173 K thermal cycling and heat-treatment testing. The columnar structure was retained after thermal cycling between 300 and 1873 K. At high temperatures between 300 and 1973–2173 K thermal cycling, the columnar grain structure was replaced by dense equiaxed grains and the grain size increased with time and temperature. The structure obtained contains pores going outwards from the coating after thermal cycling between 300 and 1873 K; on the other hand, high-temperature thermal cycling porosities were diminished. Transmission electron microscopy of the specimens showed very little difference in grain size between as-deposited coatings and those thermally cycled between 300 and 1873 K. X-ray diffraction analysis indicated that the preferred orientation of columnar structure was destroyed by thermal cycling. In addition, there was no loss in weight after thermal cycling and heat treatment testing in nitrogen.

1. Introduction

The refractory metal iridium is a candidate material as a barrier coating for carbonaceous substrates during oxidation at high temperatures, because it melts at 2713 K, has a very low oxygen permeability up to 2373 K, is non-reactive with carbon below 2553 K, and is an effective barrier to carbon diffusion [1–3]. Iridium coatings can be deposited by a wide variety of processes, i.e. chemical vapour deposition (CVD), physical vapour deposition (PVD), etc. [4]. The iridium coatings deposited by r.f. sputtering showed a better result than d.c. sputtering, due to its high throwing power, magnetic fields which confine the plasma, high deposition rate, relatively good coating uniformity and strong adhesion to the substrate, and also the formation of a dense structure after high-temperature heat treatment [5, 6]. The r.f.-sputtered iridium coatings were cracked when deposited at 1073 K owing to the mismatch in the properties of the coating and the substrate with the coefficient of thermal expansion (CTE $< 3.8 \times 10^{-6}\ K^{-1}$ at RT). For substrates with a coefficient of thermal expansion, CTE $> 5.5 \times 10^{-6}\ K^{-1}$ at RT, no cracking and good adhesion before and after high-temperature heat treatment for short times were observed, in spite of the coatings being thermally stressed [6]. The requirements of the iridium coatings are a good adhesion to the substrate, a good thermal stability at the working temperature of 1873–2173 K, a dense microstructure and long-term operation at such high temperatures. To our knowledge, no literature concerning the thermal cycling of iridium coatings is available. In view of this, the present paper reports the effect of thermal cycling and long-term heat treatment on microstructural changes of iridium coatings on isotropic graphite.

2. Experimental procedure

The iridium coatings were deposited by r.f. magnetron sputtering. The substrate material used was isotropic graphite (IG) with 6% open porosity. The size of the specimens was 15 mm × 5 mm × 1 mm. Detailed descriptions of material preparation and the isotropic graphite were given previously [6]. To remove entrapped gases from the substrate, the vacuum chamber was heated to typically 1073 K for 43.2 ks (12 h). Before coating, the substrates were etched in order to clean and activate the surface. The target used was a pure iridium (99.99%) disc, 50 mm in diameter and 1 mm thick. Ultra-high-purity argon (99.999%) was used as a sputtering gas. Prior to deposition, the target was cleaned by argon ion bombardment with the substrate shielded. The iridium coatings were deposited using the processing conditions given in Table I. The specimens were only coated on the front side. After sputtering with iridium, the specimens were allowed to cool to ambient temperature in vacuum. A coating thickness of 5–10 μm was expected to be adequate for this study.

Thermal cycling and heat treatment of the coated specimens were conducted in an electric furnace in a nitrogen atmosphere. Specimens were placed on a graphite specimen holder and cycled from 5–50 times between 300 and up to 2173 K. The hold time at the maximum temperature was 1.8 ks. The average heating and cooling rates of the specimens were 5.25

0022–2461

TABLE I Sputtering conditions

Process parameter	Range
Sputtering gas	Pure Ar
Base pressure	1.6×10^{-3} Pa
Sputtering gas pressure	0.933 Pa
R.f. power	200 W (etching 100 W × 60 s)
Target to substrate spacing	40 mm
Substrate temperature	RT (about 323 K) and 1073 K
Final thickness of substrate	1 mm
Deposition rate	1 nm s^{-1}

and 2.61 K s^{-1}, respectively. The specimens were also isothermally heat treated at 1873 K for 14.4–90 ks (4–25 h) in nitrogen and 1773 K for 90 ks (25 h) in stagnant air. The specimens were weighed before and after testing.

Microstructural features of the coating surfaces and fractured cross-sections were studied using a scanning electron microscope (SEM) (Hitachi S-640) equipped with a Kevex microanalyst 7500 energy-dispersive X-ray analysis (EDX) capabilities. The thickness of the coatings was also measured from scanning electron micrographs. The crystallographic structure was determined using X-ray diffractometer (Jeol DX-QERP 12) operated at 30 kV and 20 mA with CuK_α radiation. Transmission electron microscopy (TEM) studies and selected-area electron diffraction were carried out using a Jeol JEM-200B operated at 200 kV. The TEM specimens were ground from the graphite side to a thickness of about 100 μm. After dimpling to a depth of 70–80 μm, the specimens were ion milled and the ion beam was maintained at 25° until a thin, electron-transparent region was obtained.

3. Results and discussion

The scanning electron micrographs (Fig. 1) show microstructural features of the iridium coatings deposited on isotropic graphite at 1073 K. Fig. 1a shows the cross-section of a fracture surface of the as-deposited specimen. The thickness of the iridium coating is ≈ 8 μm. The as-deposited iridium coatings contain columnar grains oriented in the direction perpendicular to the substrate. The other noteworthy feature is the absence of porosity at the columnar boundaries. The microstructures of the as-deposited specimens contained no sputtering gas, as confirmed by energy dispersive X-ray (EDX) analysis. Furthermore, graphite is a porous material and a significant amount of porosity can be seen in the substrate, Fig. 1a, arrowed.

Fig. 1b, an enlarged view of the marked area in Fig. 1a, shows that the columnar grains and distinct grain boundaries are present. The coating consisted of densely packed columns. Fig. 1c shows that the surface morphology of the coating was smooth. Scanning electron microscopy (SEM) studies also revealed that the coating contained no pores. The columnar structure of the iridium coating makes it very strain tolerant and gives it a smooth finish. The results also show that no cracks were formed, in spite of the differences

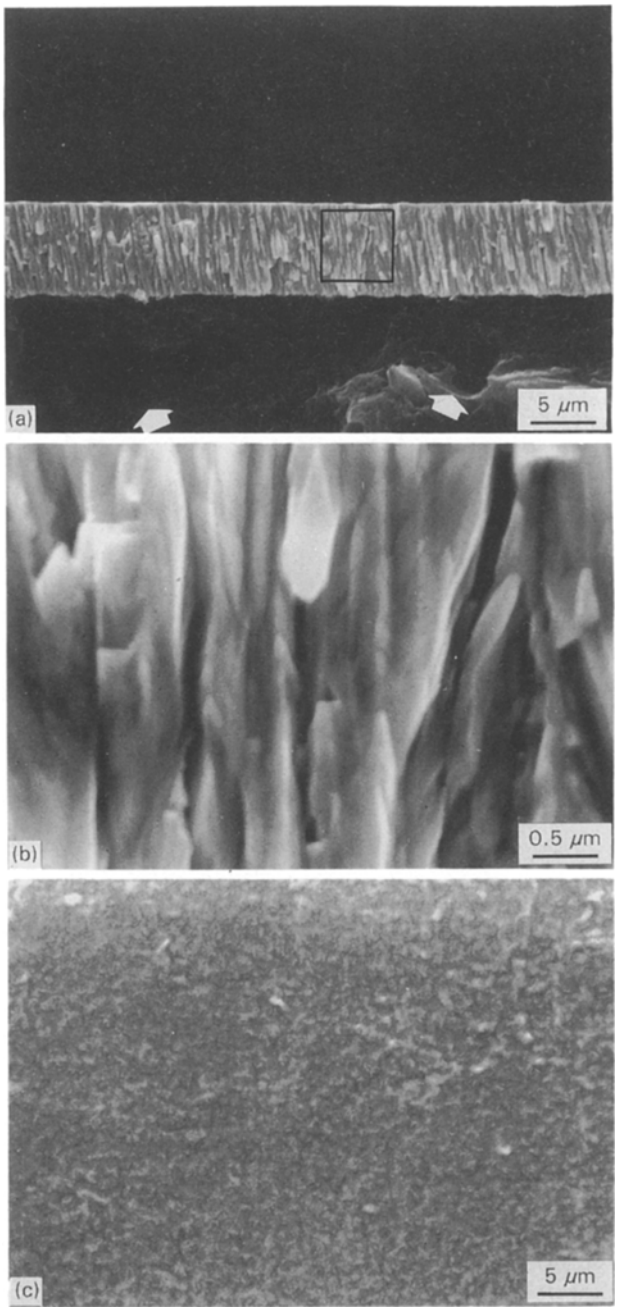

Figure 1 Scanning electron micrographs of as-deposited iridium coatings on isotropic graphite: (a) cross-sectional view of the fracture surface, (b) higher magnification image of box region of (a), and (c) surface view. (Arrows show porosities in the graphite substrate.)

in the values of the thermal expansion (α (iridium) ≈ 6.4×10^{-6} K^{-1}; α(IG) ≈ $5.8 \pm 0.9 \times 10^{-6}$ K^{-1} at 293 K). It is possible to calculate the thermally induced stresses if the expansion coefficients and the difference between the deposition and measurement temperatures, are known. The as-deposited coatings possesed a residual thermal stress of about 290 MPa [6]. Transmission electron micrographs of as-deposited iridium coating show an average grain size of iridium to be about 0.25 μm (Fig. 2).

Cross-sections of the fracture surfaces of the coatings are illustrated in Fig. 3a–d which are a sequence for thermal cycles between 300 and 1873 K. The microstructures of the iridium coating after 5, 10, 25 and 50 thermal cycles show that the columnar grains are still

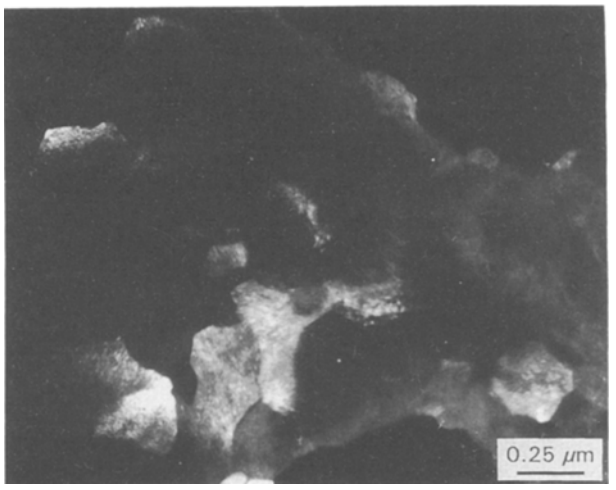

Figure 2 TEM dark-field image of as-deposited iridium coatings.

present within the coatings. Pores are easily seen now, going outwards from the coating and the severity of the porosity increases after 25 and 50 thermal cycles, whereas no pores are evident in the as-deposited structure, as shown in Fig. 1a and b. For 5 thermal cycles, crystallized granular grains embedded in the grooves of isotropic graphite of about 0.4 μm thick at the coating–substrate interface, are well defined (Fig. 3a, arrowed). Similar changes occurred in a coating which was thermally cycled 10 times, but is somewhat more pronounced in Fig. 3b. Comparable, but more noticeable, changes occurred at the coating–substrate interface after 25 and 50 thermal cycles where the thickness of the granular grain layers were about 1.2 and 2 μm, respectively, Fig. 3c and d. It seems this may be due to the diffusion of iridium into the pores, macro- and micro-roughness, which were present on the substrate surface. They provide sites for the columnar structure to coalesce and to be depleted, and for granular grains to form to decrease the surface energy. Fig. 3e also show entrapped spherical or elongated pores, whereas open boundaries were diminished. Fig. 3a–d show that the columnar structure is retained and the iridium coating is still firmly bonded to graphite after thermal cycling between 300 and 1873 K.

The surface morphologies of coated specimens subjected to thermal cycle testing between 300 and 1873 K are shown in Fig. 4a–d. After 5 and 10 thermal cycles, a slight change was seen in the surface morphology, but no cracks were observed. This can be observed by comparing the microstructures of Figs 1c, 4a and b. However, after 25 and 50 thermal cycles, the surface of the iridium coating appears to be relatively porous and pores are clearly visible, in contrast with as-deposited coatings. A comparison of Fig. 4a–d shows that the density of the pores increased with increasing number of thermal cycles. No cracking nor spallation of the coatings was observed, although the thermal stress due to the coefficient of thermal expansion mismatch is of the order of about 1.8 GPa at 300–1873 K, calculated from the model proposed by Lang *et al.* [7].

After thermal cycling, the coating–substrate interface remained well defined. The coating thickness during thermal cycle testing (Fig. 3a–d) had slightly increased. These increases in coating thickness seem to be due to outward diffusion of gases accompanied by the iridium diffusion, leading to an increase in volume and hence coating thickness. Figs 3 and 4 clearly show no channelling of the pores in the coating. No weight loss was observed after thermal cycle testing of the specimens.

Fig. 5 shows transmission electron micrographs of a coating thermally cycled 50 times between 300 and 1873 K. The bright-field image Fig. 5 clearly show dislocation-free grains of iridium with an average grain size of about 0.35 μm and well-defined grain boundaries. The microstructural features of the as-deposited coating shown in Fig. 2a are the same as in

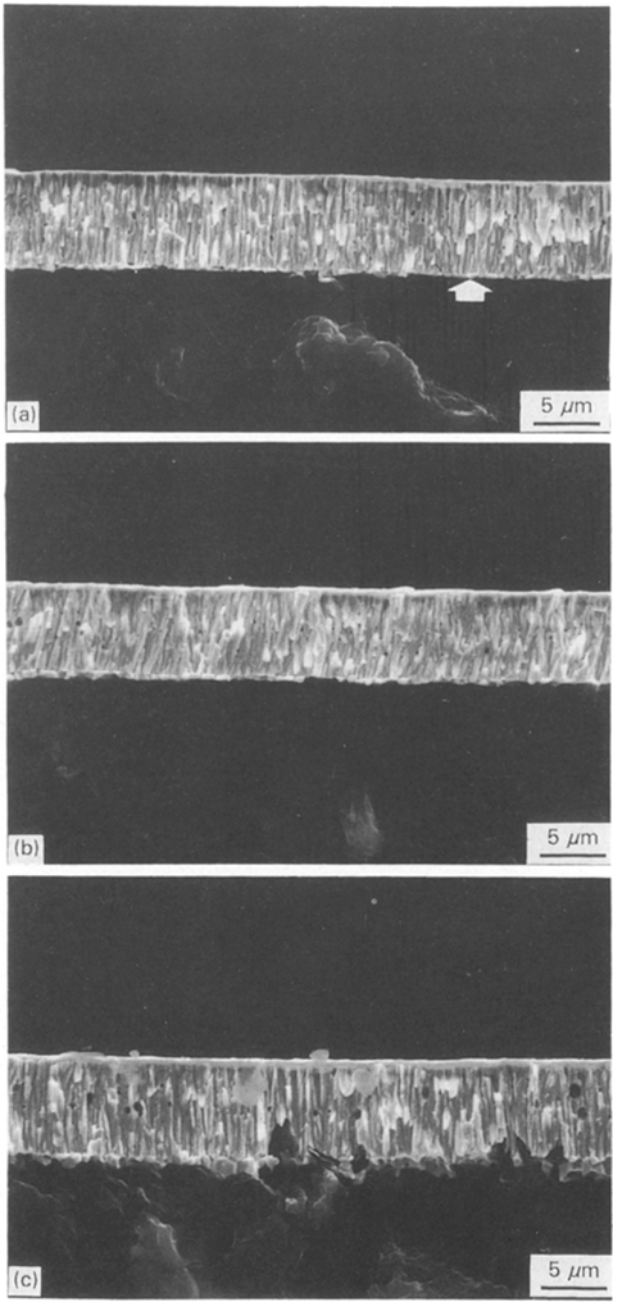

Figure 3 SEM cross-sectional micrographs of iridium coatings subjected to thermal cycling between 300 and 1873 K: (a) 5 cycles, (b) 10 cycles, (c) 25 cycles, (d) 50 cycles; (e) higher magnification image of the area marked in (d).

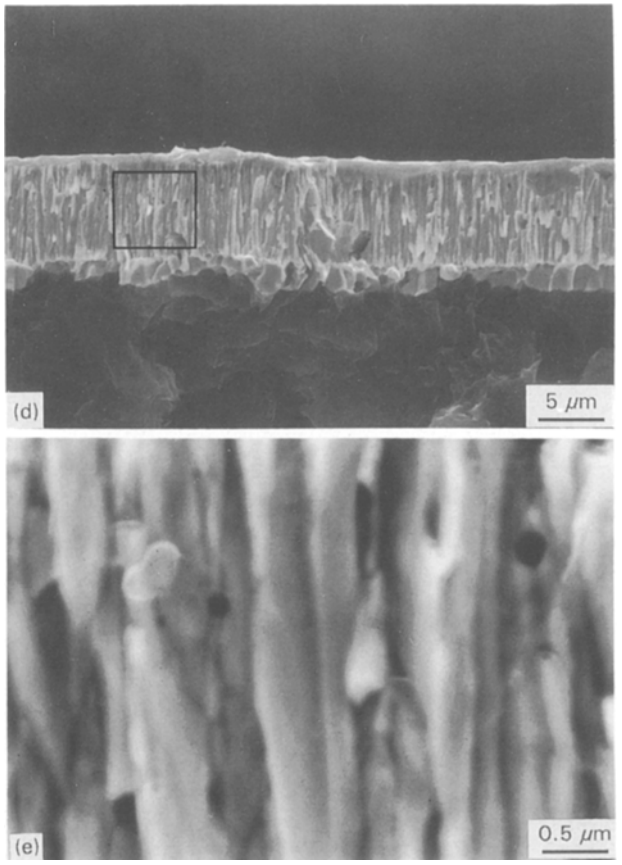

Figure 3 (continued).

Fig. 5a, and there was little difference in the grain size of the iridium coatings.

The SEM cross-sectional micrographs in Fig. 6 were taken from the specimens after they had been cycled 25 times between 300 and 1973–2173 K. Fig. 6a and b shows that the columnar grain structures were replaced by granular grains. However, entrapped pores are still present in the coating, and a few pores are seen between coating and substrate. The temperature 1973 K was sufficient to replace the columnar grain structure by granular grain structure after 1.8 ks heating. Additionally, all thermally cycled specimens showed no spalling and no degradation of adhesion at either edge or corner. Cracking was not observed, even though the calculated stresses on the coating between 300 and 1973 K and between 300 and 2173 K were about 3.9 and 5.4 GPa, respectively [7]. Fig. 6a and b also show pores and cavities at the interface. It is notable in Fig. 6a and b that the coating has a rough surface morphology. It seems that the deformation of grains occurred during heating due to the thermal stress, and the shape was distorted somewhat by gravitational effects. Furthermore, deviation from the spherical shape of the grain to the irregular shape may be because the surface-free energy can vary significantly with surface orientation as a consequence of the specific crystallographic arrangements of atoms near different surfaces [8]. All the specimens show that the iridium coatings remained adherent to the substrate after high-temperature thermal cycling.

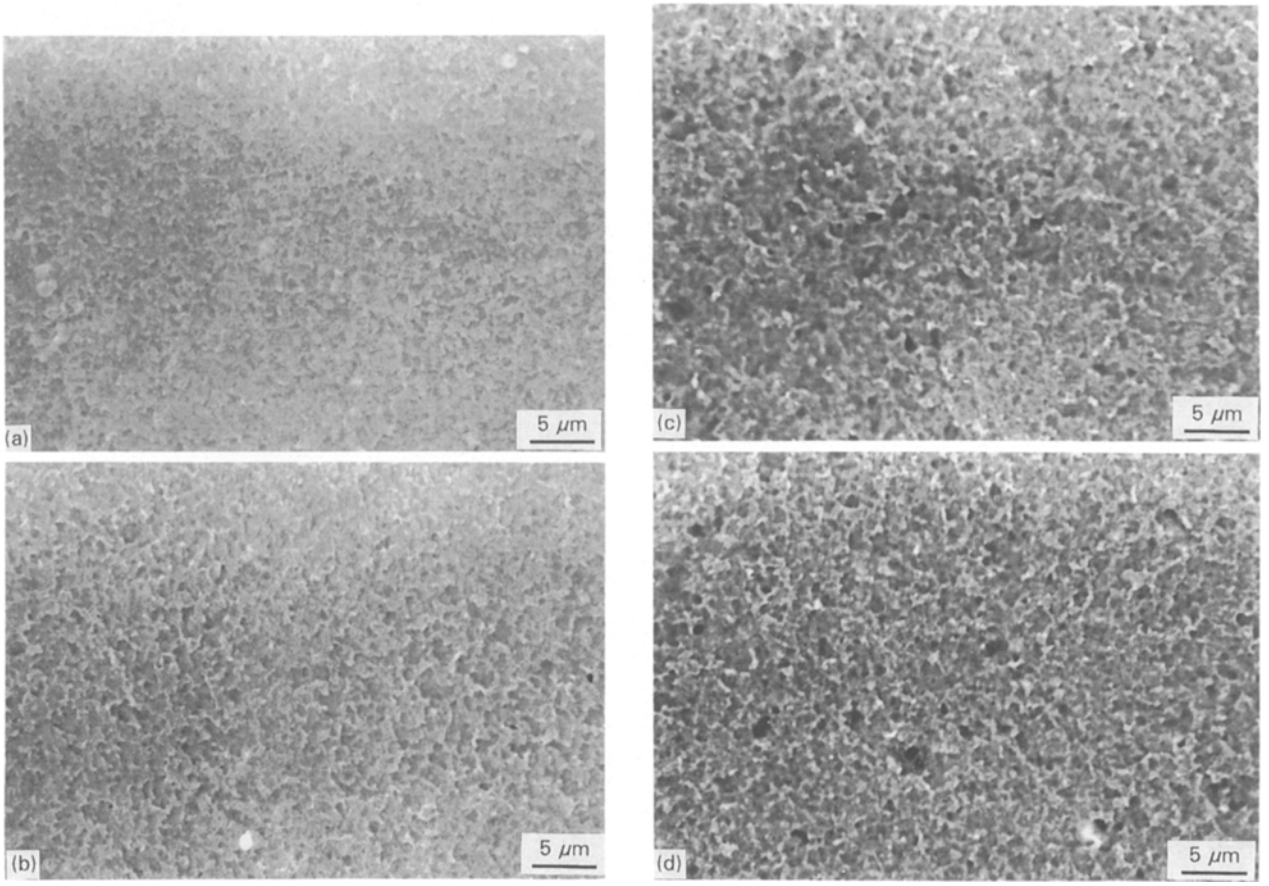

Figure 4 SEM surface micrographs of iridium coatings subjected to thermal cycling between 300 and 1873 K: (a) 5 cycles, (b) 10 cycles, (c) 25 cycles and (d) 50 cycles.

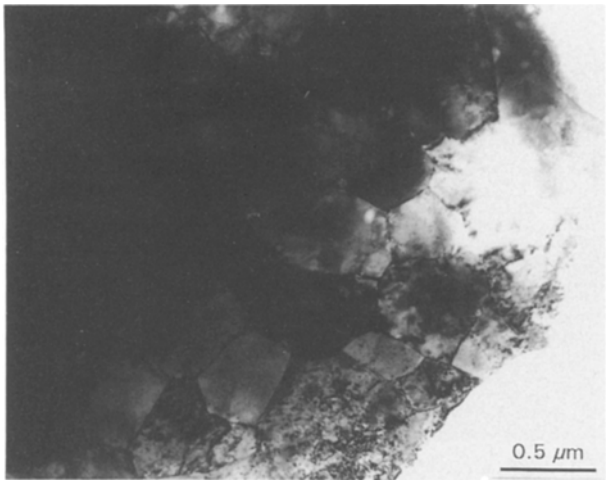

Figure 5 TEM bright-field image of iridium coatings after 50 thermal cycles between 300 and 1873 K.

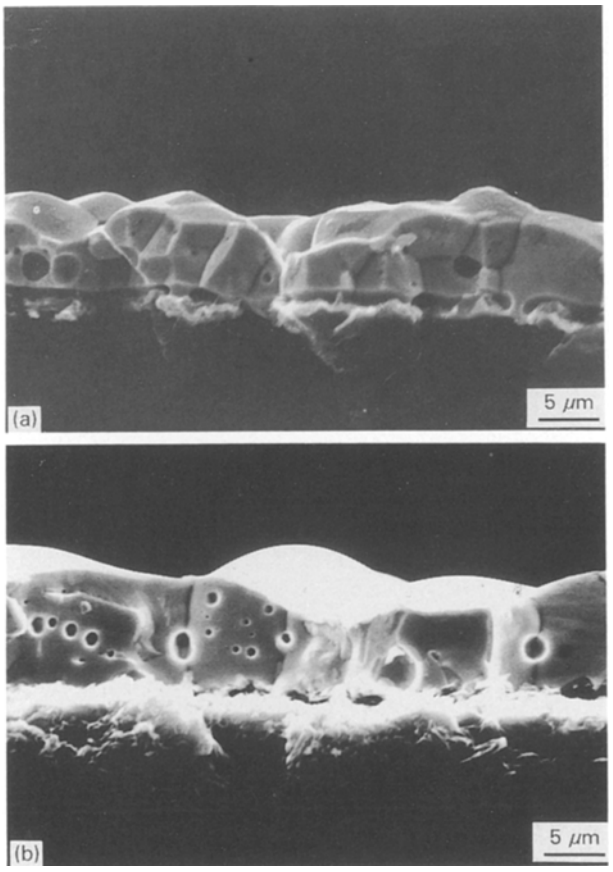

Figure 6 SEM cross-sectional micrographs of iridium coatings after 25 thermal cycles: (a) between 300 and 1973 K and (b) between 300 and 2173 K.

Comparison of Figs 4c and 7a also reveals that the voids were formed in the coatings, but not so frequently in the coatings which were thermally cycled at higher temperature. According to Fig. 7a and b the number of pores diminished after 25 cycles between 300 and 1973 K and between 300 and 2173 K, and the average grain sizes were about 10 and 25 μm, respectively. It seems that thermal cycling at these temperatures reduces the induction time and increased the grain-growth rate [9]. The temperatures (1973 and

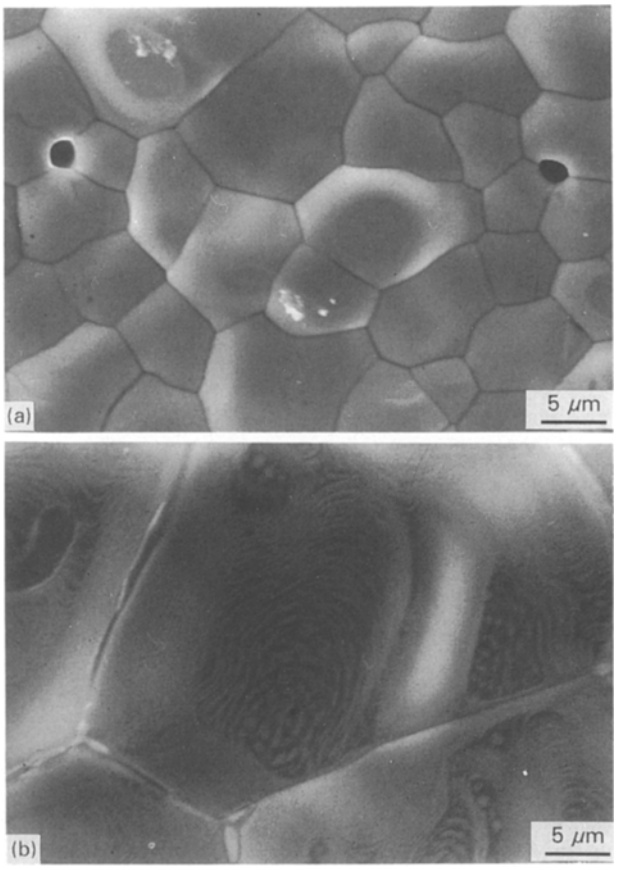

Figure 7 SEM surface micrographs of iridium coatings after 25 thermal cycles: (a) between 300 and 1973 K and (b) between 300 and 2173 K.

2173 K) were high enough to allow rapid atomic mobility of iridium, resulting in grain growth. In Fig. 7b, some white areas are visible at the grain boundaries junction; EDX analysis confirmed that these areas are iridium only and the cross-section EDX analysis indicated no formation of any compound at the coating–substrate interface.

Fig. 8 compares the cross-sectional and surface microstructures of iridium coatings after continuous heating at 1873 K in nitrogen for 14.4, 28.8 and 90 ks. Several points are noteworthy with regard to the microstructures in Fig. 8a–c. The specimen that was heat treated for 14.4 ks still has a columnar structure and a thin layer of granular grains of iridium was formed at the interface, Fig. 8a. The specimen that was heat treated for 28.8 and 90 ks has undergone structural changes, Fig. 8b and c, shows complete lack of columnar grain structure within the coating and instead dense granular grains are formed. The transition from columnar grains to granular grains occurred between 14.4 and 28.8 ks continuous heat treatment at 1873 K. The corresponding surface micrographs show that coarsening of the grains occurred, Fig. 8d–f. Fig. 8e and f reveal irregular-shaped granular structure, the size of the grains becoming larger with increasing heating time. The pores were still randomly located throughout the microstructure, and exhibited a near spherical morphology. The diameter of these pores increased with increasing heating time but the number of pores decreased. No evidence of

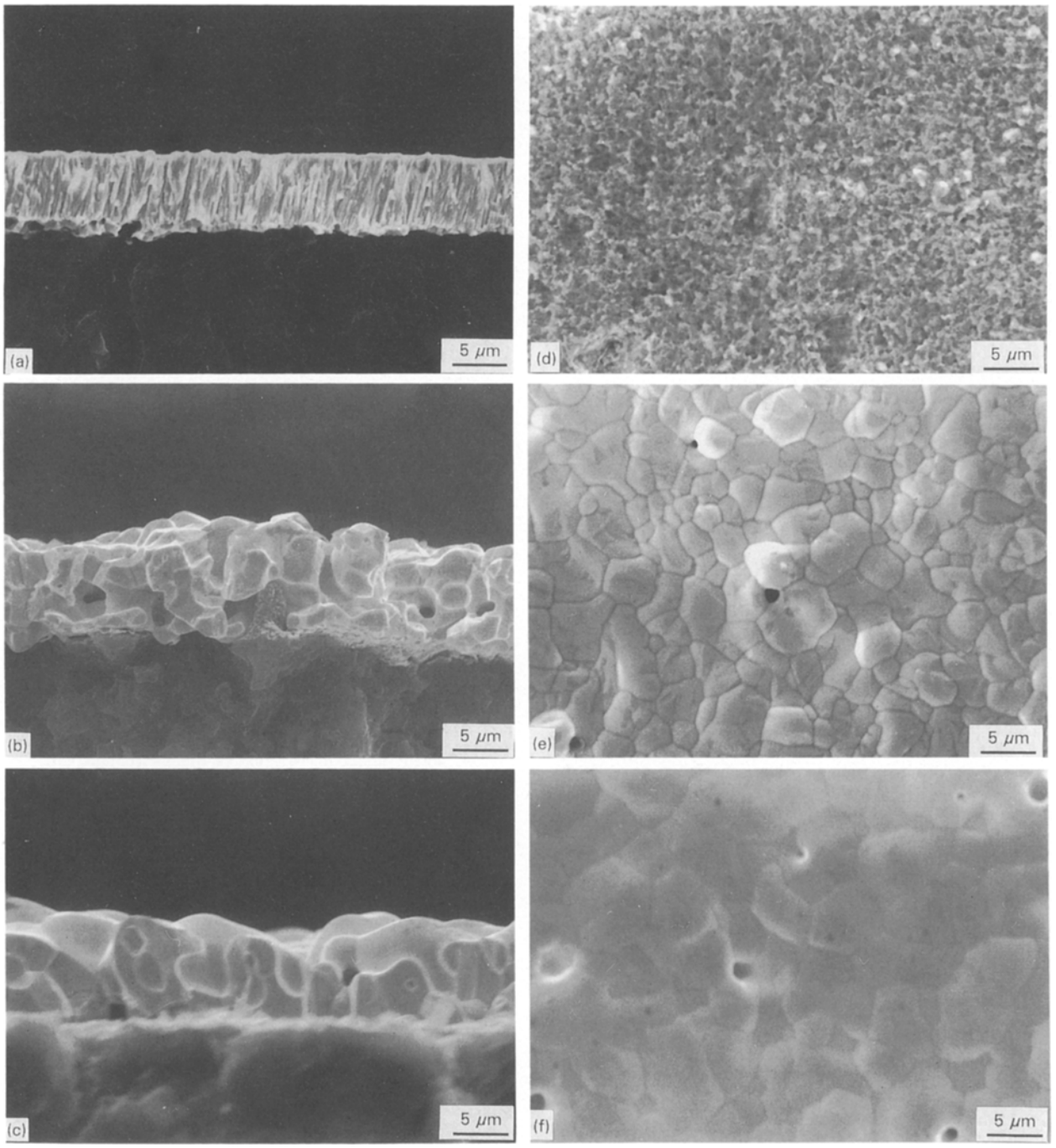

Figure 8 (a–c) Cross-sectional and (d–f) surface scanning electron micrographs of iridium coatings after continuous heat treatment at 1873 K in a nitrogen atmosphere for (a, d) 14.4 ks, (b, c) 28.8 ks, and (c, f) 90 ks.

microcracking was observed and the coating remained intact with the substrate after continuous heating for a long time. Fig. 9 shows the effect of heating time on the average grain size of iridium coating after continuous heating at 1873 K. It is seen that the crystallite sizes obtained at 1873 K after 14.4 ks heat treatment are ≈ 0.6 μm, which is nearly the same as that of the as-deposited coating. Fig. 9 clearly shows that a heat treatment shorter than 14.4 ks does not change the grain size. Continuous heating for a long time (90 ks) increases the grain size about 10 times. Prolonged heating of the coating resulted in grain coarsening, in which grains commence to grow by devouring the neighbouring fine grain, which, in itself, exhibits a stability towards normal grain growth. Because atomic rearrangements are controlled by diffusion, this means that the formation of the granular grains must be a time-dependent, thermally activated process.

An investigation by thermal cycling and heat treatment of iridium coatings has shown that the coating structure is markedly dependent on time and temperature. The formation and growth of pores during high-temperature thermal cycling or heat treatment may also be associated with a mass imbalance due to diffusion of the iridium atoms from the coating. The removal of iridium atoms results in the creation of vacancies. These vacancies accumulated in the coating, resulting in the formation of pores. In addition, at elevated temperatures, vacancies would be expected to be annihilated. Nevertheless, a moving grain boundary or other interface might be expected to be a suitable sink for a vacancy [9]. The formation of pores is

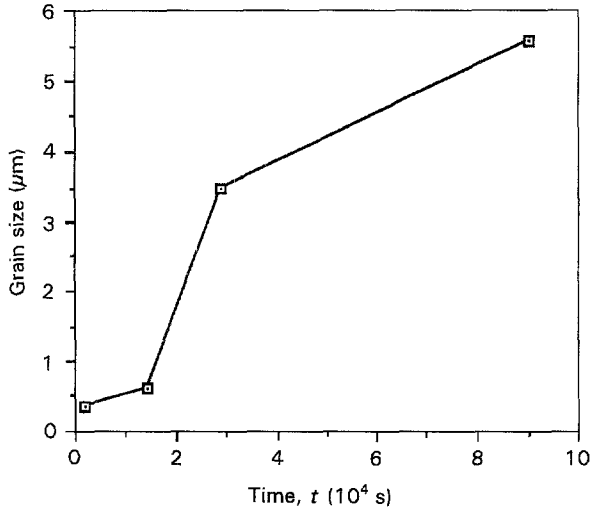

Figure 9 A plot of the average grain size versus time for the iridium coating after continuous heat treatment at 1873 K.

a thermally activated process involving the preferential diffusion of iridium. The differences in the diffusion rates of iridium with temperature affect the kinetics of pore formation. It was observed that as the grain size of the iridium increases both with time and temperature, the average number of pores decreases due to the coalescence of smaller pores into larger pores. The size and number of these pores were dependent on the temperature and exposure time.

Fig. 10 shows scanning electron micrographs of iridium coatings after heat treatment at 1773 K for

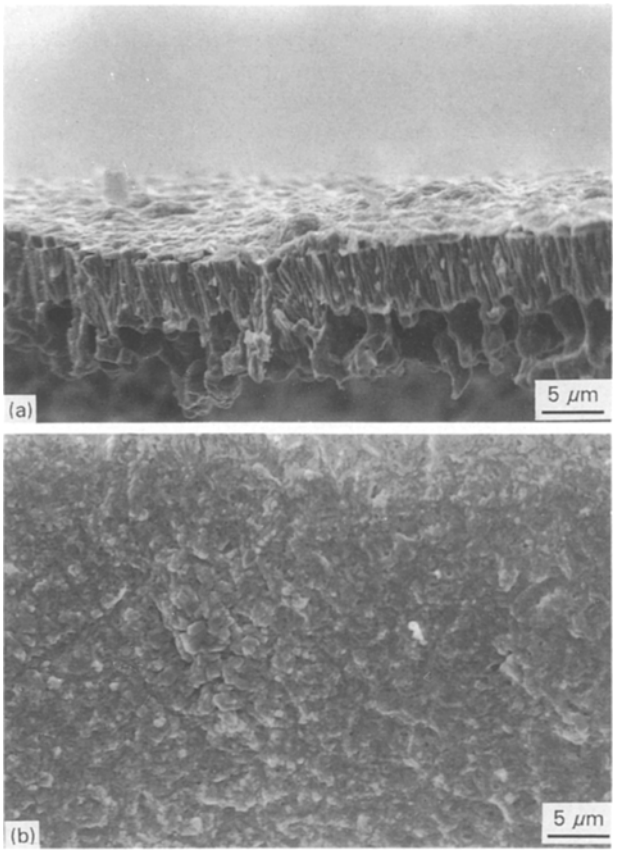

Figure 10 Scanning electron micrographs of iridium coatings after heat treatment at 1773 K for 90 ks in stagnant air: (a) cross-sectional view, (b) surface view.

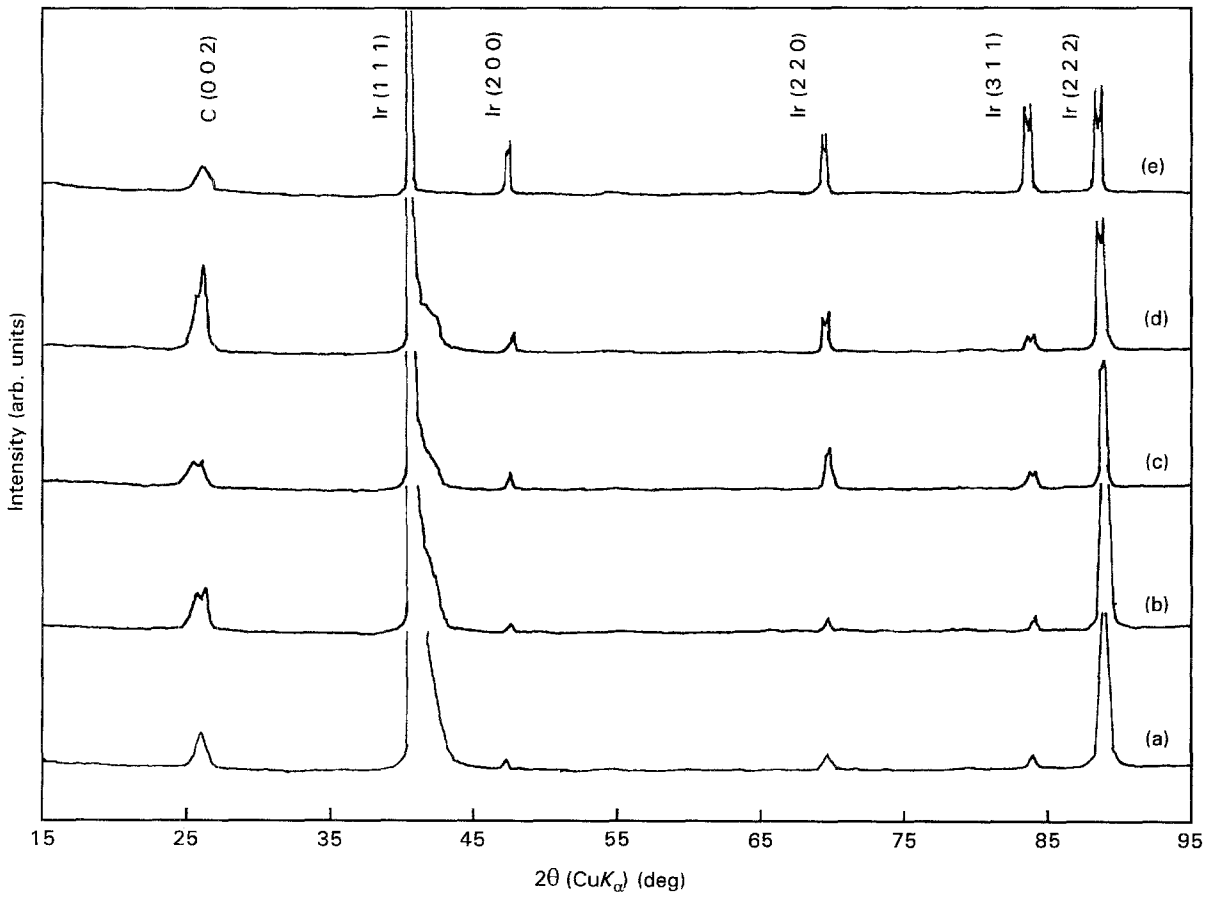

Figure 11 XRD patterns of iridium coatings after thermal cycling between 300 and 1873 K: (a) as-deposited, (b) 5 cycles, (c) 10 cycles, (d) 25 cycles and (e) 50 cycles.

90 ks in stagnant air. Iridium is not expected to form a protective oxide coating; however, gaseous oxides, mostly IrO_2 and Ir_2O_3, were identified above 1273 K [10, 11]. Once oxygen reached the reaction site, it first combined with carbon to form CO or CO_2 Fig. 10a, a cross-sectional micrograph, clearly shows three zones. On the surface a thin layer can be seen which is only iridium coating. In the intermediate zone, columnar structure remained, and at the bottom of the coating, larger grains are formed. Under these conditions the graphite was completely oxidized. It seems that the oxygen partial pressure, was not high enough to oxidize the iridium coating; instead selective oxidation of the graphite substrate occurred. The elongated grain structure may be due to the penetration of iridium into the porous graphite substrate. Preliminary testing in stagnant air has shown that coatings can survive after 90 ks (25 h) continuous heating at 1773 K. Fig. 10b shows the still dense columnar structure. It should be noted that the diffusion of iridium into the graphite pores helps to improve the adhesion of the coating.

The results of the X-ray diffraction analyses of as-deposited coatings and coatings thermally cycled between 300 and 1873 K are shown in Fig. 11. The XRD peaks from the face of all the specimens are shown, so that the preferred orientation may be distinguished. The diffraction pattern in Fig. 11a exhibits the broad diffraction line produced by the as-deposited coating. These lines become narrower for specimens after an increase in the number of thermal cycles (Fig. 11b–e), indicating recrystallization in the coatings. XRD analysis indicated that with the increase in the number of thermal cycles the degree of crystallinity increases in the coating. According to XRD diffraction analyses shown in Fig. 11, as-deposited and thermally cycled specimens produced microstructures exhibiting four dominant peaks, i.e. (1 1 1), (2 0 0), (2 2 0) and (3 1 1) [12]. The results show that the development of a highly preferred (1 1 1) texture of as-deposited coating was completely destroyed with increase in time and temperature, and changed into equiaxial grains with random orientation. This may be caused by the graphite substrate orientation without any preferred orientation.

4. Conclusions

From the above results and microscopic observation, we may conclude that r.f.-sputtered iridium coatings show considerable promise, demonstrating a tolerance to thermal cycling and continuous heat treatment for long times. All the thermally cycled and heat-treated coatings showed good adherence to the graphite substrate and no cracks in spite of the differences in the values of thermal expansion. The crystallinity and microstructure of the coatings varied with time, temperature and number of thermal cycles. The crystallinity in the coatings increased with number of thermal cycles. Columnar grain structure was retained in the coatings and a granular grain layer was formed at the interface after thermal cycling between 300 and 1873 K, whereas columnar grain structure was replaced by equiaxed grains at high-temperature thermal cycling or continuous heating at 1873 K for 90 ks. Pores were also reduced or diminished after high-temperature thermal cycling.

Acknowledgements

The authors thank Dr T. Matsuyama, Toshiba Ceramics Company Ltd, for providing the different types of graphites, and Nissan Aerospace and Kashima Oil Company, for their support.

References

1. J. R. STRIFE and J. E. SHEEHAN, *Ceram. Bull.* **67** (1988) 369.
2. W. G. MOFFATT, "The Handbook of Binary Phase Diagrams" (Genium Schenectady, NY, 1981).
3. E. M. SAVITSKII, "Handbook of Precious Metals" (Hemisphere, New York, 1981).
4. J. R. STRIFE and J. G. SMEGGIL, *J. Am. Ceram. Soc.* **73** (1990) 838.
5. K. MUMTAZ, J. ECHIGOYA and M. TAYA, *J. Mater. Sci.* **28** (1993) 5521.
6. K. MUMTAZ, J. ECHIGOYA, T. HIRAI and Y. SHINDO, *Mater. Sci. Eng. A* **167** (1993) 187.
7. G. A. LANG, B. J. FEHDER and W. D. WILLIAMS, *IEEE Trans. Electron Devices* **ED 17** (1970) 787.
8. K. H. BEHRNDT, *Thin Solid Films* **7** (1971) 415.
9. L. E. MURR, "Interfacial Phenomena in Metals and Alloys" (Addison-Wesley Advanced Book Program, Reading, MA, 1975).
10. R. T. WIMBER and H. G. KRAUS, *Metal. Trans.* **5** (1974) 1565.
11. S. N. TRIPATHI and M. S. CHANDRASEKHARAIAH, *High Temp. Sci.* **17** (1984) 365.
12. Joint Committee on Powder Diffraction Standards, 6-0598.

Received 22 June 1993
and accepted 5 July 1994